Amplified Spontaneous Emission and Lasing in Colloidal Nanoplatelets

Burak Guzelturk,[†,§,⊥] Yusuf Kelestemur,[†,⊥] Murat Olutas,[†,‡] Savas Delikanli,[†] and Hilmi Volkan Demir[†,§,*]

[†]Department of Electrical and Electronics Engineering and Department of Physics, UNAM, Institute of Materials Science and Nanotechnology, Bilkent University, Ankara 06800, Turkey, [‡]Department of Physics, Abant Izzet Baysal University, Bolu 14280, Turkey, and [§]Luminous! Center of Excellence for Semiconductor Lighting and Displays, School of Electrical and Electronic Engineering, School of Physical and Materials Sciences, Nanyang Technological University, 639798 Singapore. [⊥]These authors contributed equally to this work.

ABSTRACT Colloidal nanoplatelets (NPLs) have recently emerged as favorable light-emitting materials, which also show great potential as optical gain media due to their remarkable optical properties. In this work, we systematically investigate the optical gain performance of CdSe core and CdSe/CdS core/crown NPLs having different CdS crown size with one- and two-photon absorption pumping. The core/crown NPLs exhibit enhanced gain performance as compared to the core-only NPLs due to increased absorption cross section and the efficient interexciton funneling, which is from the CdS crown to the CdSe core. One- and two-photon absorption pumped amplified spontaneous emission thresholds are found as low as 41 μJ/cm^2 and 4.48 mJ/cm^2, respectively. These thresholds surpass the best reported optical gain performance of the state-of-the-art colloidal nanocrystals (*i.e.*, quantum dots, nanorods, *etc.*) emitting in the same spectral range as the NPLs. Moreover, gain coefficient of the NPLs is measured as high as 650 cm^{-1}, which is 4-fold larger than the best reported gain coefficient of the colloidal quantum dots. Finally, we demonstrate a two-photon absorption pumped vertical cavity surface emitting laser of the NPLs with a lasing threshold as low as 2.49 mJ/cm^2. These excellent results are attributed to the superior properties of the NPLs as optical gain media.

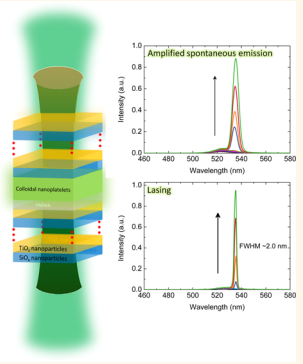

KEYWORDS: amplified spontaneous emission · colloidal nanoplatelets · vertical cavity surface-emitting laser · optical gain

Colloidal quantum dots (QDs) have been considered as versatile and promising light-emitting materials toward achieving full color lasers.[1,2] However, optical gain is severely limited in these colloidal nanocrystals due to the nonradiative Auger recombination.[3,4] Alternatively, various shaped nanocrystals, including nanorods and tetrapods, were developed and shown to achieve more efficient optical gain than the QDs.[5−10] Yet, the maximum reachable gain was still restrained in these materials.[6] Recently, colloidal nanoplatelets (NPLs), which are also known as colloidal quantum wells, have been introduced.[11−13] The NPLs exhibit superior optical and electronic properties as compared to the QDs, including their narrower spontaneous emission spectra, suppressed inhomogeneous emission broadening, and giant oscillatory strength, which are highly desired for optical gain and lasing applications.[14−16] In addition, with the great efforts in recent years, the syntheses of NPLs having different thicknesses are optimized[12] and NPLs having assorted structures such as core/crown (laterally grown shell)[16,17] and core/shell (vertically grown shell) are synthesized with higher quantum yield and stability and larger absorption cross section.[18]

Among these, CdSe/CdS core/crown NPLs (or also denoted as CdSe/CdS nanoheteroplatelets with CdS wings) are highly attractive due to their photophysical properties. First, the peak emission wavelength of the core/crown NPLs does not change (except a few nanometer red shift) as compared to their core-only counterparts owing to the confinement of the excitons in the core, where the excitons are mainly recombined. Second, core/crown NPLs preserve their narrow spontaneous emission properties of the core-only NPLs, while the absorption cross section of the NPL is boosted due to the interenergy transfer from the crown to the core.[16,17] Third, with the growth of CdS crown, the quantum yield and stability of the NPLs are enhanced.[17] With these attractive properties, core/crown NPLs were proposed to be promising for photovoltaic devices.[16]

* Address correspondence to volkan@bilkent.edu.tr, hvdemir@ntu.edu.sg.

Received for review April 23, 2014 and accepted May 31, 2014.

Published online 10.1021/nn5022296

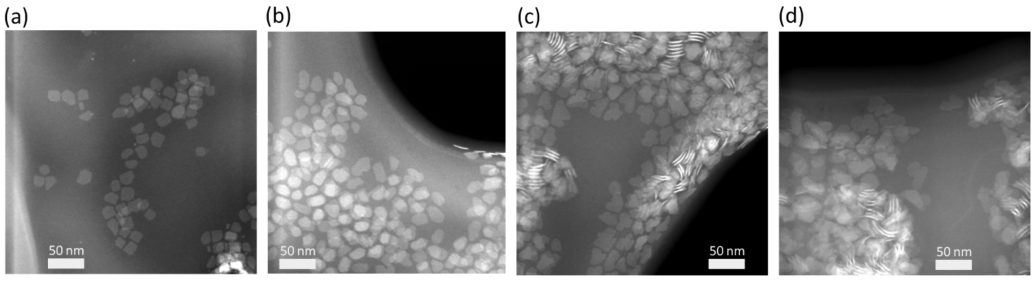

Figure 1. HAADF-TEM images of (a) core-only and core/crown NPLs having a size of (b) 21, (c) 25, and (d) 32 nm.

Furthermore, light-emitting diodes of the NPLs were demonstrated.[19] To date, however, optical gain performances of the NPLs have not been investigated. During the review process of our work, the report by Talapin *et al.* appeared to show the one-photon absorption pumped amplified spontaneous emission in core and core/shell NPLs.[20] However, neither two-photon absorption pumped amplified spontaneous emission nor lasing was reported in these newly emerging NPLs.

In this work, we report one- and two-photon absorption (1PA and 2PA) pumped amplified spontaneous emission (ASE) in core-only and varying crown size core/crown NPLs for the first time. Core/crown NPLs demonstrate substantially enhanced 1PA and 2PA pumped ASE performance as compared to the core-only NPLs. Among the varying size core/crown NPLs, the NPLs with thicker crown size exhibit better ASE performance as compared to the thinner ones. However, as the crown thickness is further increased, the shape of the NPLs becomes irregular; thus, ASE performance is deteriorated possibly due to the increase of the number of defects. The 2PA and 1PA pumped ASE thresholds are as low as 4.5 mJ/cm^2 and 41 μJ/cm^2, respectively. The ASE performance of the NPLs surpasses that of the best reported QDs and other shaped nanocrystals emitting in the same spectral range. Gain coefficient of the core/crown NPLs is measured as high as 650 cm^{-1}, which is 4-fold larger than that of the best reported QD-based gain media and also outperforms that of the other shaped nanocrystals. The superior performance of the NPLs is attributed to advantageous properties including the interexciton funneling from the CdS crown into the CdSe core and suppressed Auger recombination.[15,16] Finally, we demonstrate a 2PA pumped vertical cavity surface-emitting laser of the core/crown NPLs with a lasing threshold of ~2.49 mJ/cm^2.

RESULTS AND DISCUSSION

We synthesize four monolayer (4 ML) thick CdSe core and CdSe/CdS core/crown NPL layers having different crown size with the modified recipe.[17] Briefly, CdSe/CdS core/crown NPLs are synthesized in two steps. As compared to a single-step synthesis of core/crown NPLs, two-step synthesis results in highly uniform NPLs with reproducible results. First, 4 ML CdSe NPLs are synthesized with an emission at 515 nm. Second, after purification of the 4 ML CdSe NPLs, the CdS crown layer is grown with the injection of cadmium and sulfur precursors at higher temperature. The synthesis of the core and core/crown NPLs is explained in the Experimental Section in detail. Figure 1 depicts high-angle annular dark-field transmission electron microscopy (HAADF-TEM) images of the core-only and three different crown size core/crown NPLs. The core-only NPL has a shape varying between square and rectangle with average long-edge length of 16.8 nm (Figure 1a) with a standard deviation of 2.28 nm. For the core/crown NPLs, simply by changing the injection amount of cadmium and sulfur precursors, we can tune the size of the crown layer. Therefore, by changing the injection amounts, we achieve core/crown NPLs having the average size of 20.6, 25.3, and 31.9 nm with standard deviations of 4.29, 5.00, and 5.27 nm, as shown in Figure 1b–d, respectively. In the case of core/crown NPLs, the vertical thickness is the same thickness as the initial CdSe NPLs due to only lateral growth of the CdS crown. It is also worth mentioning that, as the crown layer grows larger, the shape of the NPLs starts to become more irregular and nonuniform as can be seen for 25 and 32 nm size core/crown NPLs (see Figure 1c, d).[17]

Figure 2a shows the absorbance and photoluminescence (PL) spectra of the core and the varying crown size core/crown NPLs. The core/crown NPLs are denoted by their average long-axis length as 21, 25, and 32 nm. As shown in Figure 2a, spontaneous emission peak of the NPLs appears at 515 and 517 nm for the core-only and core/crown NPLs, respectively. The slight red shift of the spontaneous emission by 2 nm in the case of core/crown NPLs is possibly due to the change of the dielectric medium of the excitons and induced strain by the CdS crown layer. Absorbance of the core only and core/crown exhibits the heavy- and light-hole transitions at 513 and 480 nm, respectively. In the case of core-only NPLs, the absorption around 400 nm is flat. However, a new absorption peak at 407 nm starts to arise and becomes more prominent as the CdS crown is grown larger. This peak is due to the first exciton peak of the CdS layer having 4 ML thickness, which also supports the formation of the CdS crown.[16]

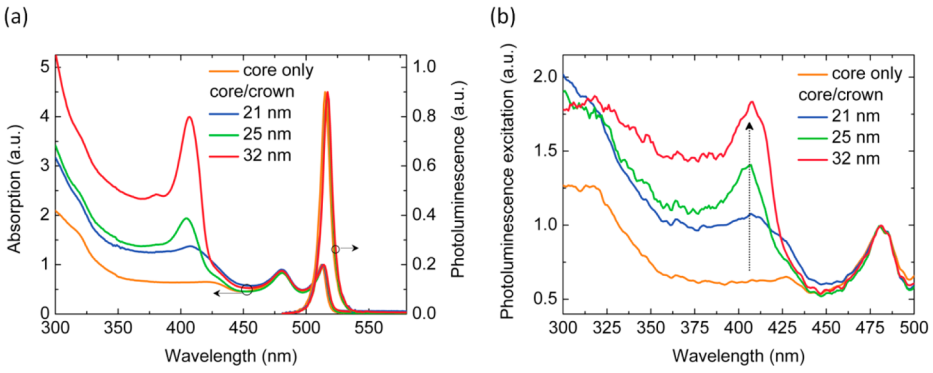

Figure 2. (a) Absorbance and photoluminescence of the NPLs: core only (orange), core/crown NPL having size of 21 nm (blue), 25 nm (green), and 32 nm (red). (b) Photoluminescence excitation spectra of the core-only and core/crown NPLs.

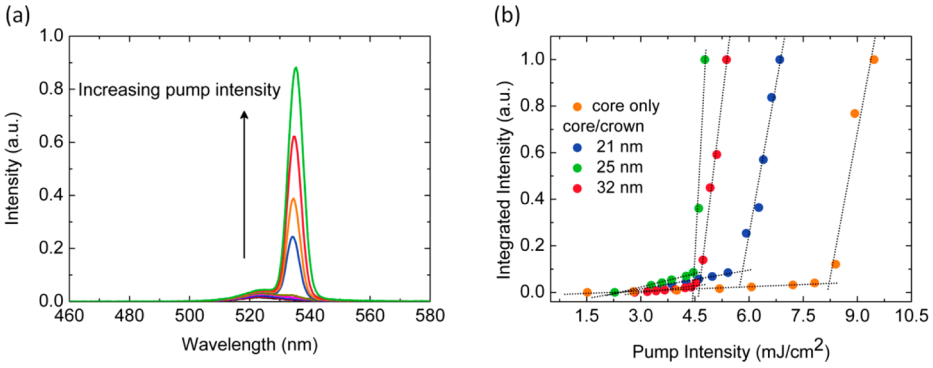

Figure 3. (a) 2PA pumped ASE of the 21 nm size core/crown NPLs. (b) 2PA pumped luminescence *vs* pump intensity of the core-only and core/crown NPLs having a size of 21, 25, and 32 nm.

Figure 2b shows the photoluminescence excitation (PLE) spectra of these NPLs that are measured for their peak emission wavelength at 515 nm (core only) and 517 (core/crown). The PLE spectrum of the NPLs resembles their absorption spectrum. In the case of core/crown NPLs, CdS's first exciton absorption peak at 407 nm also emerges in the PLE spectrum, which indicates that CdS crown strongly transfers its exciton to the CdSe core.[16] This type of efficient exciton funneling, which substantially enhances the absorbance of the nanocrystals, was observed in the core/shell QDs and nanorods.[21−24] In our case, inter-NPL exciton funneling is expected to boost the absorbance of the NPLs in the spectral range that covers the first exciton absorption peak of the 4 ML CdS crown (λ < 407 nm).[16,17] Pump lasers, which are generally mode-locked femtosecond lasers of Ti:sapphire crystals, generally operate at around 800 nm (or ~400 nm when frequency-doubled). Therefore, enhancing the optical absorption at the wavelength of the conventional high-power pump lasers will result in increased exciton density in the core/crown NPLs reducing the threshold for the population inversion condition.

To study the amplified spontaneous emission in these NPLs, we prepare close-packed solid films by drop-casting them on precleaned glass substrates. The details of the ASE experiments can be found in the Experimental Section. In the case of 2PA pumped ASE (λ_{ex} = 800 nm), luminescence spectra of the ~21 nm sized core/crown NPLs are shown as an exemplary case in Figure 3a for increasing pump intensity (see Supporting Information Figure S1 for the other NPLs). At low pump intensities, spontaneous emission dominates the PL spectra of the NPLs with full width at half-maxima (fwhm) of 18−20 nm in solid films of the NPLs. As the pump intensity is increased further, an ASE peak arises in the emission spectrum at ~534 nm having a narrower fwhm of ~5 nm. For the NPLs investigated here, the position of the ASE peak is red-shifted by 12−13 nm as compared to the spontaneous emission peak. This highly red-shifted ASE peak indicates the existence of multiexciton gain which was shown to be common for type-I-like QDs.[25] Moreover, owing to very small Stokes shift (2 nm) of these NPLs, the red-shifted ASE in these materials is highly desired that contributes to decreased self-absorption and, thus, enhanced optical gain performance.

Figure 3b demonstrates the integrated emission intensity *versus* pump intensity for the core-only and the varying crown size core/crown NPLs. The ASE thresholds for 2PA pumped are 8.21, 5.81, 4.48, and 4.63 mJ/cm^2 for the core-only, 21, 25, and 32 nm core/crown NPLs, respectively. The core/crown NPLs demonstrate substantially lowered ASE thresholds as

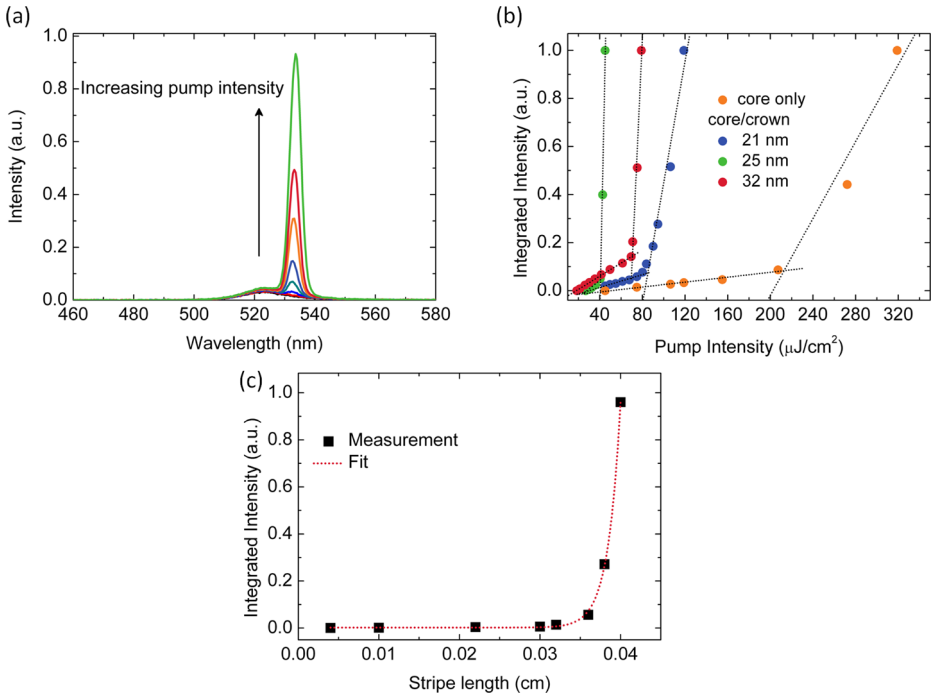

Figure 4. (a) 1PA pumped ASE of the 21 nm size core/crown NPLs. (b) 1PA pumped luminescence *vs* pump intensity of the core-only and core/crown NPLs having a size of 21, 25, and 32 nm. (c) Variable stripe length measurement of the gain coefficient.

compared to the core-only NPLs. We interpret the substantial reduction of the ASE threshold in the core/crown NPLs owing to the enhanced absorption cross section of the NPLs due to the CdS crown layer, which acts as an exciton-transferring antenna. Among the core/crown NPLs, the 25 nm one exhibits the best 2PA pumped ASE performance. The rise of the ASE threshold in the 32 nm core/crown NPLs is possibly attributed to the increased defects (indented NPLs in Figure 1d) that may quench the interenergy transfer from the crown to the core. The achieved lowest threshold of 4.4 mJ/cm^2 is a record for the spectral range of green emission, and it is ~5-fold smaller than the best reported 2PA pumped ASE threshold of the QDs that emit in the same spectral range.[26,27] Previously, this inter-NPL energy transfer from the crown layer to the core was demonstrated *via* photoluminescence excitation spectroscopy.[16] Here, we do not observe any emission from the CdS crown layer. This indicates that the inter-NPL exciton funneling is much faster than the lifetime of the ASE process, where the ASE process has the lifetime of <100 ps.[2] This type of ultrafast exciton funneling was reported for the CdSe/CdS nanorods, where CdS rod was shown to act like an antenna transferring excitons to the CdSe seeds.[22,24] Overall, the core/crown NPLs are promising candidates for frequency up-converted lasers.

Then, we investigate the 1PA pumped ASE of the NPLs (λ_{ex} = 400 nm). Luminescence spectra are plotted in Figure 4a for the 21 nm sized core/crown NPLs as an exemplary case measured for increasing pump intensities (see Figure S2 for the other NPLs). The appearance of the ASE peak is clear for the pump intensities above the 1PA pumped ASE threshold. The ASE peak is red-shifted by 10−11 nm as compared to the spontaneous emission peak. The amount of the red shift is slightly less (~2 nm) in 1PA pumped ASE as compared to the shift observed in the 2PA pumped ASE. Therefore, the ASE peaks are slightly blue-shifted in the case of 1PA pumped ASE as compared to that of the 2PA pumped case. This could be due to heating caused by 800 nm pump or due to some other excitonic effects. Figure 4b depicts the luminescence intensity *versus* pump intensity curves for the NPLs. The ASE thresholds are 214, 85, 41, and 71 μJ/cm^2 for the core-only, 21, 25, and 32 nm core/crown NPLs, respectively. Here, 25 nm sized core/crown NPLs again exhibit the best 1PA pumped ASE performance as compared to the other samples. The largest crown size NPL of 32 nm performs worse than the 25 nm NPLs, whereas their 2PA pumped ASE performances were comparable. The reason for this observation might be due to the greater two-photon absorption cross section of the 32 nm NPLs as compared to the 25 nm NPLs. The increase of the 1PA pumped ASE threshold of the 32 nm size NPLs is possibly due to the induced shape irregularities causing an increased number of defects that may quench the inter-NPL energy transfer from the crown to the cores. Achieved best 1PA pumped ASE threshold of 41 μJ/cm^2 is an important achievement for the purpose of realizing lasing with green-emitting colloidal materials. Previously, best reported

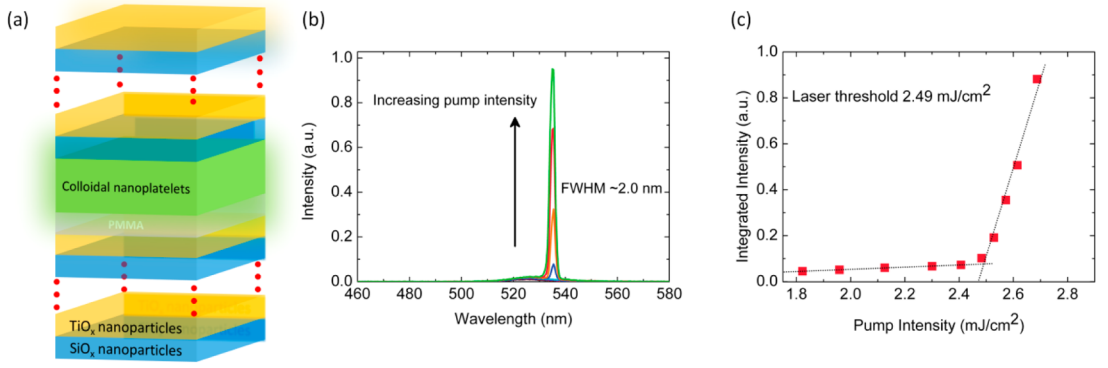

Figure 5. (a) Schematic of the VCSEL of the NPLs that employ DBRs having a six bilayer stack of SiO_2 and TiO_2 nanoparticles each. (b) Emission spectrum of the VCSEL is plotted as the pump intensity is progressively increased. (c) Integrated emission intensity *versus* pump intensity measurement and the linear fits indicating the 2PA pumped lasing threshold of 2.49 mJ/cm^2.

1PA pumped ASE threshold for the green-emitting QDs was as low as 150 μJ/cm^2.[2] Therefore, these NPLs with their record low ASE threshold levels in the green spectral emission range will be essential for achieving to the multicolor lasing (*i.e.*, R-G-B) with the colloidal materials. In addition, we perform variable stripe length (VSL) measurements to quantify the gain coefficient of the NPLs.[28,29] Figure 4c depicts the VSL measurement of the 25 nm core/crown NPL that achieves the best ASE performance both with 1PA and 2PA pumping. Surprisingly, the gain coefficient is found to be as high as 650 cm^{-1}. This gain coefficient is much greater than the best reported gain coefficients of the QDs and nanorods.[6,29] Before the best reported gain coefficient was shown to be 150 cm^{-1} in the QDs,[29] while in nanorods, it was shown be as high as 350 cm^{-1}.[6] However, this gain coefficient in nanorods could be measured only at temperatures below 120 K. Here we achieve this ultrahigh gain coefficient at room temperature. Therefore, the NPLs are proven to be excellent colloidal gain media for lasers.

Finally, we develop the proof-of-concept laser of the NPLs using all solution-processed distributed Bragg reflectors made out of alternatively stacked SiO_2 and TiO_2 nanoparticles.[30,31] Employing six bilayers of the SiO_2/TiO_2, we realize DBRs with peak reflectively as high as 91−93%. Then, we sandwich 25 nm size core/crown NPLs between two DBRs such that we realize the vertical cavity surface-emitting laser (VCSEL) of the NPLs (see Experimental Section for the details of the devices). Figure 5a illustrates the architecture of the VCSEL of the NPLs. Figure 5b shows the emission spectra of VCSELs under 2PA pumping as the pump intensity is progressively increased. After the lasing threshold, lasing peak at 535 nm emerges with a fwhm of 2 nm that corresponds to a *Q*-factor of ∼270. We observed both spectrally and spatially coherent emission from the VCSELs after the laser threshold. Figure 5c shows the luminescence intensity *versus* pump intensity plot. The threshold for the lasing is ∼2.49 mJ/cm^2. The lasing threshold is better than the 2PA pumped ASE threshold of the drop-casted 25 nm core/crown NPLs owing to the energy storage in the cavity.

CONCLUSIONS

In summary, we demonstrate that colloidal nanoplatets are promising for both 1PA and 2PA pumped optical gain and lasing. Here, for the first time, we investigate the ASE performance of the core-only and core/crown NPLs having varying crown size. These NPLs exhibit superior performance as compared to the other colloidal counterparts including QDs, nanorods, and other shaped nanocrystals. 1PA and 2PA pumped ASE thresholds of the NPLs reach record low levels at 41 μJ/cm^2 and 4.48 mJ/cm^2 for the green spectral emission region, respectively. The gain coefficient of the NPLs is measured as high as 650 cm^{-1}, which represents a 4-fold enhancement over the best reported gain coefficient of the colloidal QDs. Finally, we develop a vertical cavity surface-emitting laser of the core/crown NPLs that exhibits 2PA pumped laser with low threshold of 2.49 mJ/cm^2. These results clearly demonstrate that the NPLs are excellent materials for optical gain and lasing.

EXPERIMENTAL SECTION

Synthesis of the Four-Monolayer Core-Only and Core/Crown NPLs. The 4 ML CdSe core-only NPLs with emission at 515 nm are synthesized according to the recipe from the literature.[17] For a typical synthesis, 170 mg of cadmium myristate, 12 mg of selenium, and 15 mL of octadecene (ODE) are loaded into a three-neck flask. After evacuation of solution at room temperature, the solution is heated to 240 °C under inert atmosphere. When the temperature reaches 195 °C, the color of solution becomes yellowish. Then, 80 mg of cadmium acetate dihydrate is introduced. After 10 min growth of CdSe NPLs at 240 °C, the reaction is stopped and cooled to room temperature with the injection of 0.5 mL of oleic acid (OA). Then, 4 ML CdSe NPLs are separated by other reaction products with successive purification steps.

The synthesis of the CdSe/CdS core/crown NPL is performed with the injection of cadmium and sulfur precursors which are prepared according to recipe from the literature.[17] For a typical synthesis, certain amount of CdSe NPLs that is dissolved in hexane and 5 mL of ODE is loaded into a three-neck flask. The solution is degassed to remove all hexane, water, and oxygen inside the solution. Then, under the inert atmosphere, the solution is heated to 240 °C. When temperature reaches 240 °C, cadmium and sulfur precursors are injected with the rate of 4 mL/h. According to desired CdS crown size, injection amount can be changed. After the injection of cadmium and sulfur precursors, the reaction is stopped with the injection of 0.5 mL of OA and the system is cooled to room temperature. The CdSe/CdS core/crown NPLs are purified with successive purification steps.

Measurement of the ASE Spectra. As the optical pump source, a Spectra Physics Spitfire Pro XP regenerative amplifier having 120 fs pulse width at 800 nm with a 1 kHz repetation rate is used. A cylindirical lens (20 cm focus) is employed to excite the samples with a stripe geometry. A variable neutral density filter is used to adjust the pump intensity on the samples. Then, pump-intensity-dependent luminescence is collected *via* a fiber-coupled spectrometer (Maya2000 Pro). The collection geometry is perpendicular to the excitation pump. For the single-photon pumping, the pump source is frequency-doubled using a nonlinear BBO crystal and the residual 800 nm pump is filtered out by a high-frequency pass filter.

Fabrication of the VCSELs of the Core/Crown NPLs. SiO_2 nanoparticle solution (Aldrich Ludox TMA 30 wt %, water) and TiO_2 nanoparticle solution (Nanoamor Rutile TiO_2 nanoparticles 15 wt %, water) were diluted with ethanol to have final concentrations of 2.2 and 5 wt %, respectively. To fabricate the DBRs, we alternatively deposit the nanoparticles *via* spin-coating them at 4000 rpm for 1 min on piranha-cleaned quartz substrates. Between each deposition step, the samples are annealed at 200 °C. As an optical path separation to realize multiple available longitudinal modes, we deposit PMMA (PMMA 950 A9) with spin rate of 4000 rpm for 45 s on top of one of the DBR. Then, we drop-coat the NPLs (30−40 mg/mL) on the DBR that was not deposited with PMMA. We bring the two DBRs together, apply slight pressure, and using an epoxy we fix the formed cavity.

Conflict of Interest: The authors declare no competing financial interest.

Acknowledgment. The authors would like to thank the EU-FP7 Nanophotonics4Energy NoE, TUBITAK EEEAG 109E002, 109E004, 110E010, 110E217, NRF-RF-2009-09, NRF-CRP-6-2010-02, and A*STAR of Singapore for the financial support. H.V.D. acknowledges support from ESF-EURYI and TUBA-GEBIP.

Supporting Information Available: Additional information on the amplified spontaneous emission spectra of the other sized NPL samples pumped by one- and two-photon absorption. This material is available free of charge *via* the Internet at http://pubs.acs.org.

REFERENCES AND NOTES

1. Klimov, V. I.; Mikhailovsky, A. A.; Xu, S.; Malko, A.; Hollingsworth, J. A.; Leatherdale, C. A.; Eisler, H.; Bawendi, M. G. Quantization of Multiparticle Auger Rates in Semiconductor Quantum Dots. *Science* **2000**, *290*, 314–317.
2. Dang, C.; Lee, J.; Breen, C.; Steckel, J. S.; Coe-Sullivan, S.; Nurmikko, A. Red, Green and Blue Lasing Enabled by Single-Exciton Gain in Colloidal Quantum Dot Films. *Nat. Nanotechnol.* **2012**, *7*, 335–339.
3. Klimov, V. I. Quantization of Multiparticle Auger Rates in Semiconductor Quantum Dots. *Science* **2000**, *287*, 1011–1013.
4. Klimov, V. I. Spectral and Dynamical Properties of Multiexcitons in Semiconductor Nanocrystals. *Annu. Rev. Phys. Chem.* **2007**, *58*, 635–673.
5. Htoon, H.; Hollingworth, J. A.; Malko, A. V.; Dickerson, R.; Klimov, V. I. Light Amplification in Semiconductor Nanocrystals: Quantum Rods *versus* Quantum Dots. *Appl. Phys. Lett.* **2003**, *82*, 4776.
6. Kazes, M.; Oron, D.; Shweky, I.; Banin, U. Temperature Dependence of Optical Gain in CdSe/ZnS Quantum Rods. *J. Phys. Chem. C* **2007**, *111*, 7898–7905.
7. Haase, J.; Shinohara, S.; Mundra, P.; Risse, G.; Lyssenko, V. G.; Frob, H.; Hentschel, M.; Eychmuller, A.; Leo, K. Hemispherical Resonators with Embedded Nanocrystal Quantum Rod Emitters. *Appl. Phys. Lett.* **2010**, *97*, 211101.
8. Zavelani-Rossi, M.; Lupo, M. G.; Krahne, R.; Manna, L.; Lanzani, G. Lasing in Self-Assembled Microcavities of CdSe/CdS Core/Shell Colloidal Quantum Rods. *Nanoscale* **2010**, *2*, 931–935.
9. Moreels, I.; Rainò, G.; Gomes, R.; Hens, Z.; Stöferle, T.; Mahrt, R. F. Nearly Temperature-Independent Threshold for Amplified Spontaneous Emission in Colloidal CdSe/CdS Quantum Dot-in-Rods. *Adv. Mater.* **2012**, *24*, OP231-5.
10. Liao, Y.; Xing, G.; Mishra, N.; Sum, T. C.; Chan, Y. Low Threshold, Amplified Spontaneous Emission from Core-Seeded Semiconductor Nanotetrapods Incorporated into a Sol−Gel Matrix. *Adv. Mater.* **2012**, *24*, 159–164.
11. Ithurria, S.; Dubertret, B. Quasi 2D Colloidal CdSe Platelets with Thicknesses Controlled at the Atomic Level. *J. Am. Chem. Soc.* **2008**, *130*, 16504–16505.
12. Ithurria, S.; Bousquet, G.; Dubertret, B. Continuous Transition from 3D to 1D Confinement Observed during the Formation of CdSe Nanoplatelets. *J. Am. Chem. Soc.* **2011**, *133*, 3070–3077.
13. Ithurria, S.; Tessier, M. D.; Mahler, B.; Lobo, R. P. S. M.; Dubertret, B.; Efros, A. L. Colloidal Nanoplatelets with Two-Dimensional Electronic Structure. *Nat. Mater.* **2011**, *10*, 936–941.
14. Tessier, M. D.; Javaux, C.; Maksimovic, I.; Loriette, V.; Dubertret, B.; Kunneman, L. T.; Heuclin, H.; Aulin, Y. V.; Grozema, F. C.; Schins, J. M.; *et al.* Spectroscopy of Single CdSe Nanoplatelets. *J. Phys. Chem. Lett.* **2013**, *4*, 3574–3578.
15. Kunneman, L. T.; Tessier, M. D.; Heuclin, H.; Dubertret, B.; Aulin, Y. V.; Grozema, F. C.; Schins, J. M.; Siebbeles, L. D. A. Bimolecular Auger Recombination of Electron−Hole Pairs in Two-Dimensional CdSe and CdSe/CdZnS Core/Shell Nanoplatelets. *J. Phys. Chem. Lett.* **2013**, *4*, 3574–3578.
16. Prudnikau, A.; Chuvilin, A.; Artemyev, M. CdSe−CdS Nanoheteroplatelets with Efficient Photoexcitation of Central CdSe Region through Epitaxially Grown CdS Wings. *J. Am. Chem. Soc.* **2013**, *135*, 14476–14479.
17. Tessier, M. D.; Spinicelli, P.; Dupont, D.; Patriarche, G.; Ithurria, S.; Dubertret, B. Efficient Exciton Concentrators Built from Colloidal Core/crown CdSe/CdS Semiconductor Nanoplatelets. *Nano Lett.* **2014**, *14*, 207–213.
18. Mahler, B.; Nadal, B.; Bouet, C.; Patriarche, G.; Dubertret, B. Core/Shell Colloidal Semiconductor Nanoplatelets. *J. Am. Chem. Soc.* **2012**, *134*, 18591–18598.
19. Chen, Z.; Nadal, B.; Mahler, B.; Aubin, H.; Dubertret, B. Quasi-2D Colloidal Semiconductor Nanoplatelets for Narrow Electroluminescence. *Adv. Funct. Mater.* **2014**, *24*, 295–302.
20. She, C.; Fedin, I.; Dolzhnikov, D. S.; Demortière, A.; Schaller, R. D.; Pelton, M.; Talapin, D. V.; Richard, D. Low-Threshold Stimulated Emission Using Colloidal Quantum Wells. *Nano Lett.* **2014**, *14*, 2772–2777.
21. Kundu, J.; Ghosh, Y.; Dennis, A. M.; Htoon, H.; Hollingsworth, J. A. Giant Nanocrystal Quantum Dots: Stable Down-Conversion Phosphors That Exploit a Large Stokes Shift and Efficient Shell-to-Core Energy Relaxation. *Nano Lett.* **2012**, *12*, 3031–3037.
22. Talapin, D. V.; Nelson, J. H.; Shevchenko, E. V.; Aloni, S.; Sadtler, B.; Alivisatos, A. P. Seeded Growth of Highly Luminescent CdSe/CdS Nanoheterostructures with Rod and Tetrapod Morphologies. *Nano Lett.* **2007**, *7*, 2951–2959.
23. Talapin, D. V.; Koeppe, R.; Götzinger, S.; Kornowski, A.; Lupton, J. M.; Rogach, A. L.; Benson, O.; Feldmann, J.; Weller, H. Highly Emissive Colloidal CdSe/CdS Heterostructures of Mixed Dimensionality. *Nano Lett.* **2003**, *3*, 1677–1681.
24. Borys, N. J.; Walter, M. J.; Huang, J.; Talapin, D. V.; Lupton, J. M. The Role of Particle Morphology in Interfacial Energy

Transfer in CdSe/CdS Heterostructure Nanocrystals. *Science* **2010**, *330*, 1371–1374.
25. Klimov, V. I.; Ivanov, S. A.; Nanda, J.; Achermann, M.; Bezel, I.; McGuire, J. A.; Piryatinski, A. Single-Exciton Optical Gain in Semiconductor Nanocrystals. *Nature* **2007**, *447*, 441–446.
26. Jasieniak, J. J. J.; Fortunati, I.; Gardin, S.; Signorini, R.; Bozio, R.; Martucci, A.; Mulvaney, P. Highly Efficient Amplified Stimulated Emission from CdSe−CdS−ZnS Quantum Dot Doped Waveguides with Two-Photon Infrared Optical Pumping. *Adv. Mater.* **2008**, *20*, 69–73.
27. Zhang, C.; Zhang, F.; Zhu, T.; Cheng, A.; Xu, J.; Zhang, Q.; Mohney, S. E.; Henderson, R. H.; Wang, Y. A. Two-Photon-Pumped Lasing from Colloidal Nanocrystal Quantum Dots. *Opt. Lett.* **2008**, *33*, 2437–2439.
28. Samuel, I. D. W.; Turnbull, G. A. Organic Semiconductor Lasers. *Chem. Rev.* **2007**, *107*, 1272–1295.
29. Malko, A. V.; Mikhailovsky, A. A.; Petruska, M. A.; Hollingsworth, J. A.; Htoon, H.; Bawendi, M. G.; Klimov, V. I. From Amplified Spontaneous Emission to Microring Lasing Using Nanocrystal Quantum Dot Solids. *Appl. Phys. Lett.* **2002**, *81*, 1303.
30. Colodrero, S.; Ocaña, M.; Míguez, H. Nanoparticle-Based One-Dimensional Photonic Crystals. *Langmuir* **2008**, *24*, 4430–4434.
31. Puzzo, D. P.; Scotognella, F.; Zavelani-Rossi, M.; Sebastian, M.; Lough, A. J.; Manners, I.; Lanzani, G.; Tubino, R.; Ozin, G. A. Distributed Feedback Lasing from a Composite Poly(phenylene Vinylene)-Nanoparticle One-Dimensional Photonic Crystal. *Nano Lett.* **2009**, *9*, 4273–4278.